European Review for Medical and Pharmacological Sciences 2022; 26: 8234-8246

Screening and validation for core genes in osteoarthritic cartilage based on weighted gene co-expression network analysis

S.-Q. WANG[1], W.-P. XIE[2], L. YUE[2], Y.-L. CAI[1,2]

[1]First Clinical College, Shandong University of Traditional Chinese Medicine, Jinan, Shandong, China
[2]Department of Orthopedics, Affiliated Hospital of Shandong University of Traditional Chinese Medicine, Jinan, Shandong, China

Abstract. – OBJECTIVE: Osteoarthritis (OA) has the highest disability rate among chronic diseases. The burden on patients and public health care resources is increasingly evident due to increasing obesity rates and aging populations. So, there is still a lack of early diagnosis and treatment for OA.

MATERIALS AND METHODS: A total of three OA cartilage tissue datasets (GSE1919, GSE32317, and GSE5235) were obtained from the Gene Expression Omnibus (GEO) database. Screening of differentially expressed genes and WGCNA of overlapping genes were performed using the R language package. Functional and immune infiltration analyses of overlapping genes were also carried out while hub genes were screened through LASSO regression analysis method and ROC curve. Finally, experimental validation was carried out through PCR and Western Blot analysis of rat cartilage.

RESULTS: A total of 149 differentially expressed genes were screened, and they were mainly enriched in the cytokine-cytokine receptor interaction, rheumatoid arthritis, and interleukin (IL-17) signaling pathways. Four co-expression modules were obtained, of which the blue module was the most substantial morbidity associated with OA. Thirteen overlapping genes were identified based on significant module network topology analysis and differential genes, upon which their validation through LASSO regression analysis method and ROC curve was performed. From these, five signature genes were determined, before three potential core genes were finally identified after confirmation using the validation set.

CONCLUSIONS: ATF3, FOSL2, and GADD45B may be hub genes to the osteochondropathy, and they are expected to be new biomarkers and drug targets in OA research.

Key Words:
Osteoarthritis cartilage, Weighted gene co-expression network analysis, Differentially expressed genes, Bioinformatics analysis, Immune infiltration.

Introduction

Across the world, osteoarthritis (OA) is the most prevalent joint disease resulting in afflicting all kinds of joints throughout the body, of which the knee is the most severely affected, and morbidity increases with age[1]. Surveys have shown the prevalence is about 50% in people over the age of 60 and 80% in people over the age of 75, 2.46 times more common in women than in men, and it has a disability rate of 53%[2]. Despite the considerable individual, economic, and social costs of OA, it has not received much general attention, with some people even considering OA to be an essential part of ageing[3]. This view leads to patients often being at the end-stage of the disease when they seek medical attention and having to undergo total knee replacement. Consequently, the search for hub genes with regard to the progression of OA, and for biomarkers and targeted drugs, is of great importance in mitigating the disease's effects and reducing the disability rate of OA patients.

With the development of gene microarrays and high-throughput sequencing technologies in recent years, there has been a gradual increase in genetic data for OA. Most existing studies have focused on screening for independent differential genes, neglecting the correlation between genes and clinical phenotypes[4]. Weighted gene co-expression network analysis (WGCNA) can be performed by discovering modules of highly related genes, aggregating these modules using signature genes or hub genes within them, and association analysis either with each other or with clinical phenotypes[5,6]. This lattermost is more in line with the topological overlap measure (TOM) in a biological sense[7].

Corresponding Author: Yuli Cai, MD; e-mail: 280647730@qq.com

In this study, articular cartilage was used as an entry point to mine the GEO database for OA-related gene datasets. These datasets were then bioinformatically analyzed using WGCNA, screened and confirmed by validation groups which yielded the genes ATF3, FOSL2, and GADD45B as demonstrating the potential to be OA biomarkers and therapeutic targets. This paper provides new insights into the molecular mechanisms of osteochondropathy.

Materials and Methods

Data Collection and Preprocessing

To acquire the necessary data, the National Center for Biotechnology Information (NCBI) and Gene Expression Omnibus (GEO) database (https://www.ncbi.nlm.nih.gov/geo/) was parsed for microarray datasets by searching the keyword "osteoarthritis". This returned three datasets from cartilage tissue (GSE1919, GSE32317 and GSE55235), it contains 24 OA patients and 25 healthy control samples. The probes were annotated using Perl software (https://www.perl.org/,5.32.1.1) for the matrix file of the experimental dataset series, their names were converted into gene names, and the expression values of all probes corresponding to the same gene were averaged[8]. The "limma" package in R language was used for normalization and the "sva" package for batch correction.

Differential Gene Screening and Enrichment Analysis

The "limma" package in R language (version as per http://www.r-project.org/,4.1.2) was also used to screen the differentially expressed genes. Conditions were set at $|\log_2 FC| \geq 1$ and $p<0.05$, while the differential results were visualized with the "Pheatmap" and "ggplot2" packages. The differential genes obtained were enriched via the Kyoto Encyclopedia of GENEs and Genomes (KEGG) and Gene Ontology (GO) enrichment analysis carried out with R software.

WGCNA Construction and Module Core Gene Screening

WGCNA was performed on the processed dataset using the "WGCNA" and "limma" packages in R language. Since the index of fit was positively correlated with the power value and the average connectivity was negatively correlated with power, there was a need to find the appropriate power value[9-11]. The adjacency matrix was constructed using the proximity values between each pair of node genes in the network and their Pearson correlation coefficients, which were used to calculate the topological overlap (TOM) and the corresponding dissimilarity (1-TOM)[12]. The differences measured based on TOM were used to construct a dendrogram by clustering the mean link hierarchy to cluster highly similar modules together[13], and then merged with a height cut-off of 0.25[14]. Finally, the module with the largest absolute *p*-value was selected as the key module, and its key genes were determined by calculating its MM (Module Membership) value and GS (Gene Significance)[15,16]. The intersection genes of differentially expressed genes and core genes of WGCNA key modules were screened by VENNY 2.1 (http://bioinfogp.cnb.csic.es/tools/venny/), which mapped them out in a Venn diagram.

LASSO Regression Analysis Method and ROC Curve Validation

LASSO regression analysis method is a high-performance variable selection method which prevents activity fitting and incorporates the best prognostic factors into the modeling[17]. This method was applied, via the "glmnet" package in R language on the overlapping genes obtained in part 2.3 to screen for potential core genes. The ROC curves were then validated using the "pROC" package, and if the area under the curve (AUC) was ≥ 0.8 and $p<0.05$, the gene was considered to have a high clinical diagnostic value[18].

Immunological Cell Infiltration

CIBERSORT is a generalized deconvolution algorithm for quantifying complex tissue cell fractions from gene expression profiles[19]. For this, 28 immune cells were selected to calculate their relative proportions in the normalized gene expression data by the CIBERSORT algorithm in R software. These proportions were displayed in a bar plot function, and the Wilcoxon rank sum test was used to compare the difference in the content of each immune cell between the two groups, with $p<0.05$ used as a screening criterion for higher levels of immune infiltration. Subsequently, the results were visualized using the "vioplot" package in R language.

Experimental Validation

Experimental Animals

A total of 48 SPF-grade SD rats (6-8 weeks old, weighing 200±20 g, Jinan Panyue Laboratory Animals, Animal License No.: SCXK (Lu) 20140007) were kept on a 12-hour light-dark schedule at 25±2°C and 55%±5% humidity. They were allowed free access to food and water. These experiments conformed to the Guide for the Care and Use of Laboratory Animals published by the National Institutes of Health. All animal experiments were approved by the Animal Ethics Committee of the Affiliated Hospital of Shandong University of Traditional Chinese Medicine (AWE-2021-04).

Modeling and Experimental Administration

The rats were randomly divided into two groups: the control group and the experimental group. In the experimental group, the rats were anesthetized with 1% pentobarbital (50 mg/kg) and the left knee joints were exposed using the medial patellar approach after sterilization was performed. The anterior cruciate ligaments and medial collateral ligaments were transected, and the medial menisci were removed using the modified Hulth method to establish the KOA model. After four weeks of feeding, all rats were euthanized with 1% pentobarbital (100 mg/kg) and the knee cartilages were collected.

PCR Validation

Total RNA was extracted from rat cartilage tissues using TRlzol reagent (TaKaRa Corporation, Otsu, Shiga, Japan). 1 μg of total RNA was used as a template to configure a reverse transcription reaction system according to the protocol in the reverse transcriptase instructions. A total of 20 μL was used to synthesize cDNA. cDNA was added according to the instructions on the Fast SYBR GREEN Master Mix (Applied Biosystems, Foster City, CA, USA) kit, and the $2^{-\Delta\Delta Ct}$ method was used to calculate the gene expression levels in each of the two groups. The real-time fluorescence-based quantitative PCR primer sequences are shown in Table I.

Validation by Protein Immunoblotting

Procedure: Take about 50 mg of well separated cartilage tissue, grind and collect the bone powder, and add it into the 1000 μL RIPA lysis solution, lyse on ice for 30 min, centrifuge, transfer the supernatant to a 1.5 mL centrifuge tube, store at -20°C and then determine the protein content. Wash the glass plate, pour the gel, prepare the samples, perform electrophoresis, terminate the electrophoresis, and transfer the membrane. Allow the membranes to dry and moisturize them with TBS and then transfer to a petri dish containing the blocking buffer (5% skimmed milk powder TBST tween) and close by shaking on a decolorizing shaker (Haimen Kylin-Bell Lab Instruments Co., Ltd, Haimen, China) at room temperature for 1 hour. Incubate membranes overnight at 4°C with TBST tween containing 5% BSA diluted at 1:1,000. After incubation with TBST at 1:5,000 dilution for 2 hours at room temperature, wash the membrane 3 times for 10 minutes each in TBST on a decolorizing shaker at room temperature; perform chemiluminescence and obtain pictures through gel imaging system (Shanghai Tianneng Technology Co., Ltd, Shanghai, China).

Statistical Analysis

R4.1.2 software was utilized for the necessary statistical analysis and data processing. All measures were normally distributed using normality

Table I. The list of primer sequences in the real-time fluorescence-based quantitative PCR analysis.

Gene symbol	Primer (5′-3′)
ATF3	Forward: GAGGATTTTGCTAACCTGACACC Reverse: TTGACGGTAACTGACTCCAGC
FOSL2	Forward: CCAGCAGAAGTTCCGGGTAG Reverse: GTAGGGATGTGAGCGTGGATA
GADD45B	Forward: CAACGCGGTTCAGAAGATGC Reverse: GGTCCACATTCATCAGTTTGGC
PPP1R15A	Forward: GAGGGACGCCCACAACTTC Reverse: TTACCAGAGACAGGGGTAGGT
PTGDS	Forward: TGCAGCCCAACTTTCAACAAG Reverse: TGGTCTCACACTGGTTTTTCCT

test and expressed as: mean ± standard deviation (X±S), and differences were considered statistically significant at $p<0.05$.

Results

Gene Screening Results

A total of 149 differentially expressed genes were obtained from all datasets based on the corrected $p<0.05$ and $|\log_2 FC|\geq 1$ criteria, including 68 up-regulated and 81 down-regulated genes. The visual heat map and volcano plot are shown as per Figure 1.

Results of GO and KEGG Enrichment Analysis

GO enrichment analysis showed differentially expressed genes were mainly involved in leukocyte migration and chemotaxis, regulation of angiogenesis, and regulation of vascular system development in BP. CC enrichment showed bi-

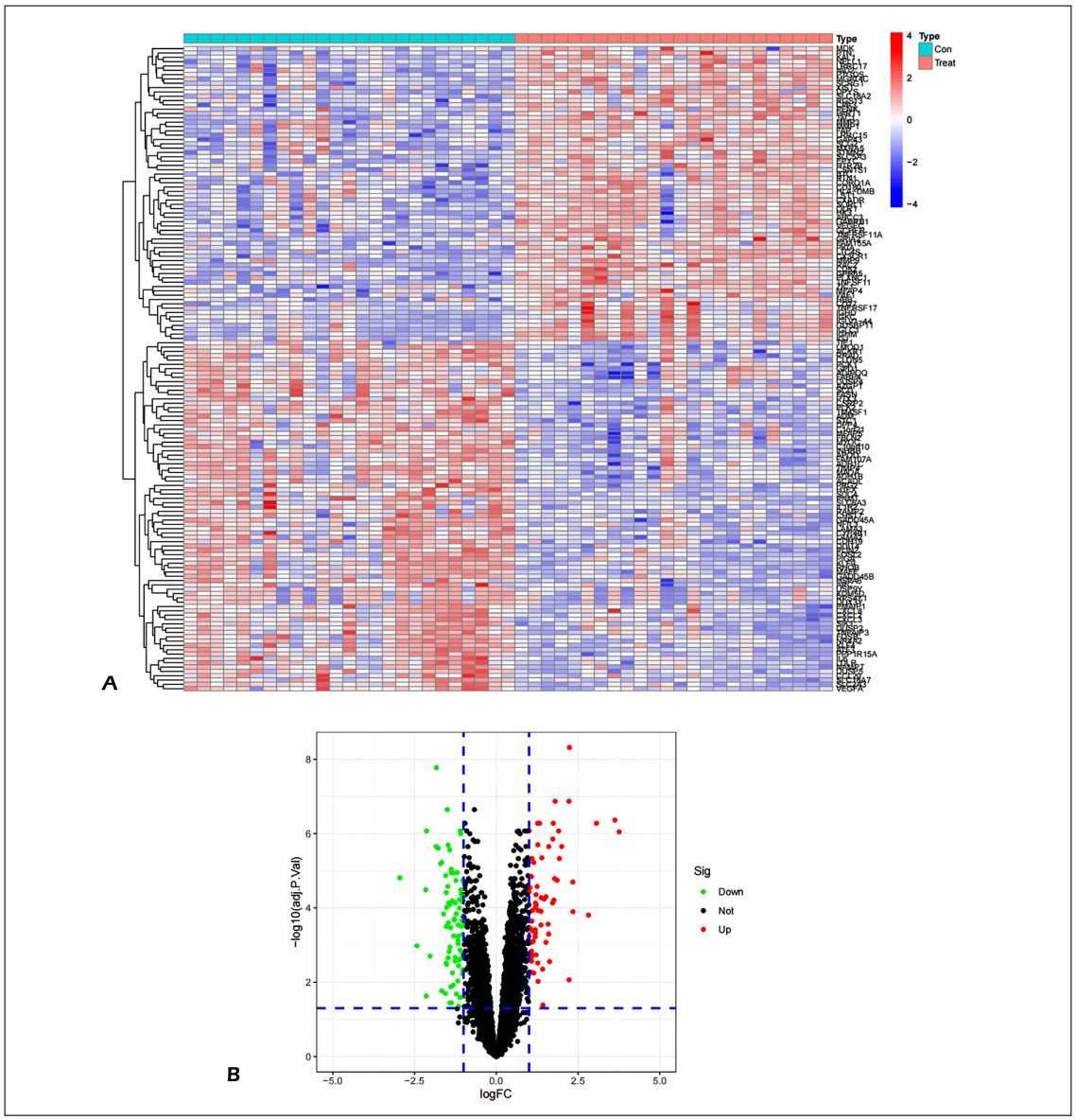

Figure 1. Screening map of OA differential genes: (**A**) heat map of the differentially expressed genes in OA and normal cartilage samples, where red represents up-regulated genes and blue the down-regulated genes, while the vertical coordinates are gene names; (**B**) volcano map of the differentially expressed genes, in which the black, red, and green parts represent genes which were not differentially expressed, upregulated genes, and down-regulated genes, respectively.

ological processes occurred mainly in the collagen-containing extracellular matrix, outer plasma membrane, etc., and in MF they were mainly enriched in receptor ligand activity, signaling receptor activator activity, and cytokine activity, as shown in Figure 2A. The KEGG pathway enrichment illustrated the enrichment of those differential genes in the cytokine-cytokine receptor interaction pathway, rheumatoid arthritis pathway, and interleukin 17 signaling pathway, as per Figure 2B.

WGCNA and Intersectional Gene Screening Results

As shown in the sample clustering (Figure 3A), there were no outliers, so no deviant samples were present to be removed when performing subsequent analyses[20]. Firstly, it was necessary to select the appropriate power value to ensure its efficacy and a standard scale-free network before conducting the analysis, as shown in Figure 3B and Figure 3C. When the power equaled 5, the correlation coefficient was 0.84, which could be considered to constitute an ideal scale-free network, at which point the scale-free topology index of fit became 0.9, which was imported into the WGCNA package to construct the gene module. The WGCNA algorithm was used to calculate the association and adjacency matrices of the gene expression profiles of the OA samples to obtain the TOM, as well as a clustering map of the genetic system and a heat map of the

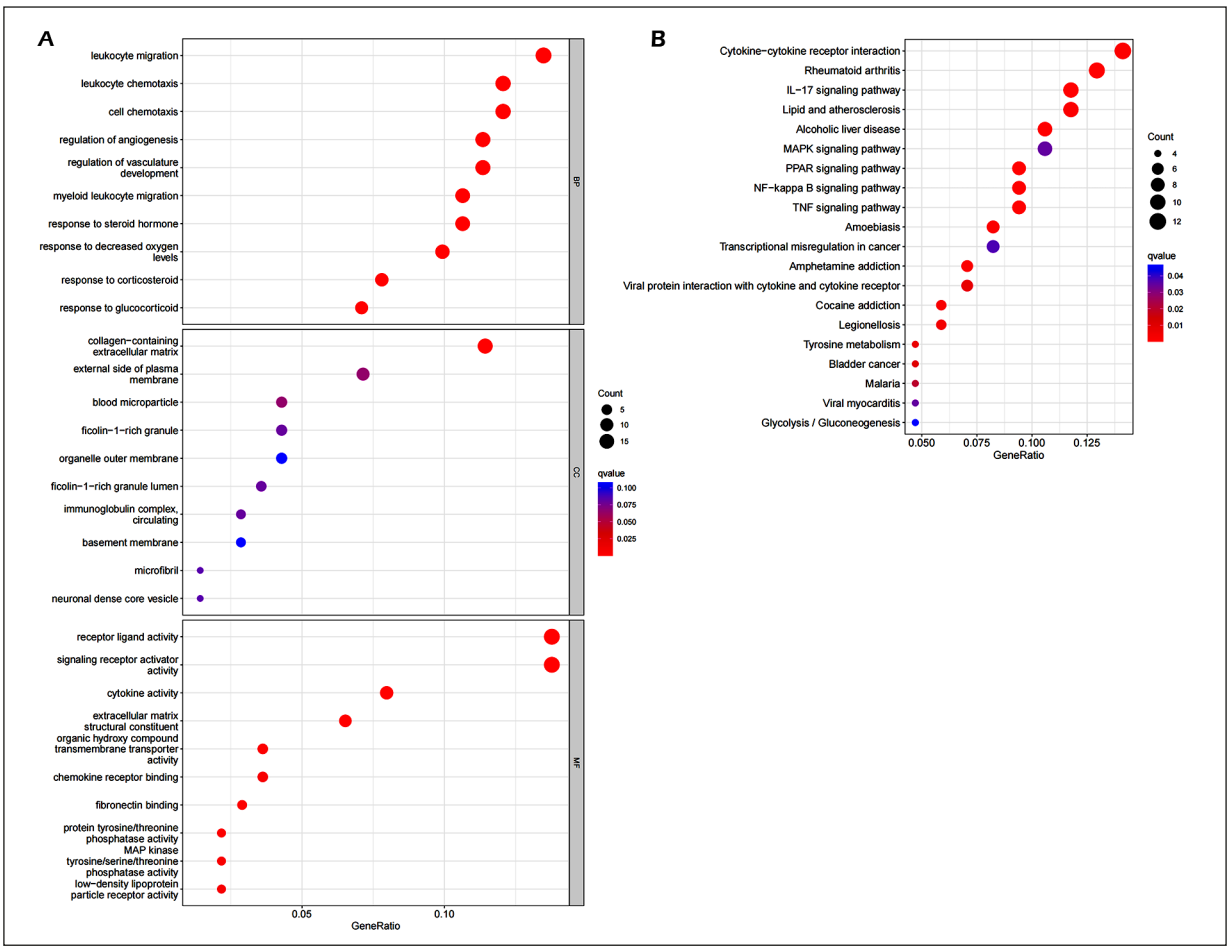

Figure 2. Plots of GO and KEGG enrichment analysis of differential genes: (**A**) GO enrichment analysis of differential genes, where the horizontal and vertical coordinates represent the rate and GO function, respectively, while the size of the dots denotes the quantity of enriched genes, (the larger the circle the more genes), and the gradient of the color indicates the corrected *p*-value (the closer to red, the smaller the *p*-value); and (**B**) KEGG enrichment analysis of differential genes, where the horizontal and vertical coordinates represent the rate and the enrichment pathway, respectively, while the size of the dots denotes the quantity of enriched genes, (the larger the circle the more genes), and the gradient of the color indicates the corrected *p*-value (the closer to red, the smaller the *p*-value).

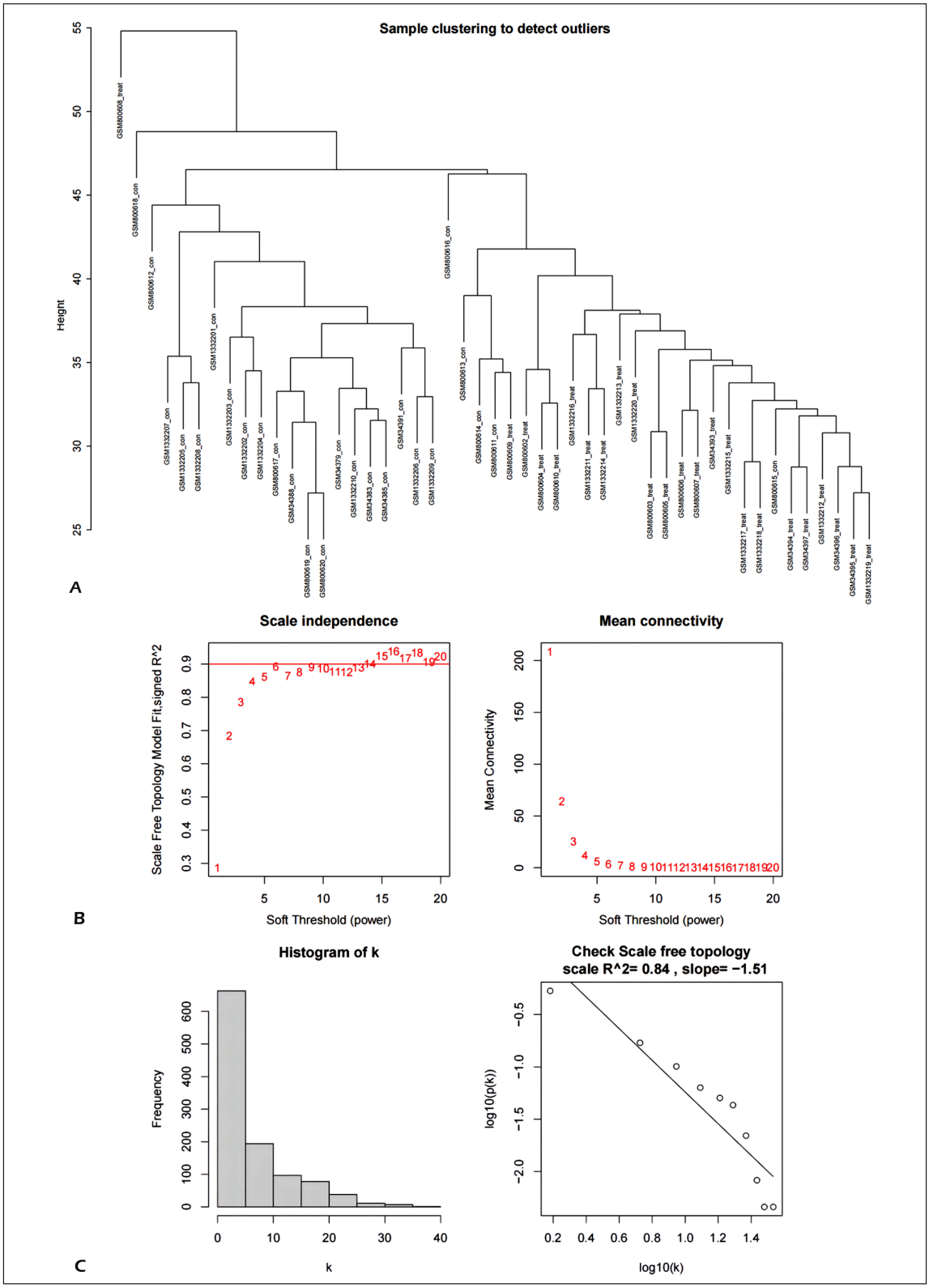

Figure 3. Sample clustering and weighted gene co-expression network pre-construction: (**A**) sample clustering showing no outliers which needed to be removed from subsequent analysis; (**B**) scale-free topology module fit with average connectivity at different soft threshold powers (β), wherein the red line in the graph on the left indicates $R^2 = 0.9$; and (**C**) test of optimal power value with a correlation coefficient of 0.84 when the power value was 5.

correlation between module features and OA (Figure 4). Through the correlation heat map, it was observed the blue module displayed the strongest positive and negative correlation with disease, containing 342 genes. To identify the core genes, an intra-module analysis was conducted on the significant modules, defining the core genes as those satisfying the conditions GS>0.5 and MM>0.8. From this, sixteen genes were obtained, as shown in Table II. A further thirteen potential genes were obtained by plotting the Venn diagram, which were then used for the next analysis, as shown in Figure 5.

LASSO Regression Analysis Method and ROC Curve Validation Results

As shown in Figure 6A-6B, five feature genes were obtained from LASSO regression analysis method, namely ATF3, FOSL2, GADD45B, PPP1R15A, and PTGDS. ROC curve analysis was performed on these five genes and screened applying the criteria of AUC≥0.8 and $p<0.05$ for testing. The results showed all five genes met these criteria, displaying good diagnostic value (Figure 6C-6G).

Immunological Cell Infiltration Results

Analysis of the proportion consisting of immune cells in the data set and the differences revealed activated B cells, macrophages, CD4 memory T cells, and memory B cells were significantly more highly expressed in OA cartilage tissue compared to normal chondrocytes, while eosinophils and CD8 memory T cells were relatively less expressed (Figure 7).

Experimental Results

PCR results showed that ATF3, FOSL2, GADD45B, PPP1R15A and PTGDS were significantly different between the two groups ($p<0.05$), (Figure 8 A-E). Western blot results showed that ATF3, FOSL2 and GADD45B were significantly different between the control and experimental groups ($p<0.05$). The differences in expression were not significant between PPP1R15A and PTGDS ($p>0.05$) (Figure 9 B-F). In consideration of the two results, we suggest that ATF3, FOSL2 and PTGDS may be the core genes of OA.

Discussion

OA is one of the common orthopedic diseases and its morbidity is increasing year by year while seriously threatening people's quality of life. In normal adult cartilage, chondrocytes are normally quiescent cells, and their survival and anabolic activity are essential for maintaining cartilage tissue. Therefore, chondrocyte metabolism has an essential influence in the pathogenesis of OA[21]. In response to the current situation in which the molecular mechanisms of OA are still unclear, in this study we used bioinformatics analysis methods to investigate OA biomarkers and pathological processes in cartilage tissue obtained from OA and normal cartilage.

In contrast to other bioinformatics analyses, WGCNA can systematically describe patterns of association between genes across microarray samples, and this approach has been successfully applied to the analysis of cancer, mouse genetic and brain imaging data[22]. The enrichment analysis revealed the differential genes obtained in the three samples from the experimental group were primarily enriched in signaling pathways related to the inflammatory response. Thus, the pathological process of OA may be mediated by inflammatory cytokines and other anti-inflammatory cytokines, and these cytokines are likely to have a protective effect on the joint tissue by modulating the inflammatory response[23]. The results of immune infiltration analysis showed macrophages and other cells are significantly upregulated in OA cartilage and may play a role in the inflammatory response to OA. It has been reported that macrophages may be involved in cartilage repair by regulating the validation response[24], which provides a new direction for our understanding of how OA progresses. Finally, ATF3 (activating transcription factor 3), FOSL2 (fos-like antigen2), and GADD45B (growth arrest and DNA-damage inducible protein beta) were screened through the test of the validation group. The result was consistent with previous enrichment analyses and immunological cell infiltration results; therefore, it is suggested that ATF3, FOSL2, and GADD45B are likely to be potential biomarkers and therapeutic targets for the treatment of OA.

ATF3 is currently recognized as a stress-inducible gene, as well as a hub gene in the cellular adaptation response[25]. It also acts as a selective marker of neuronal injury and is often highly expressed as neuropathic pain caused by peripheral nerve injury[26], which may be related to the painful symptoms of OA. Blom et al[27] observed increased expression of ATF3 in a mouse model

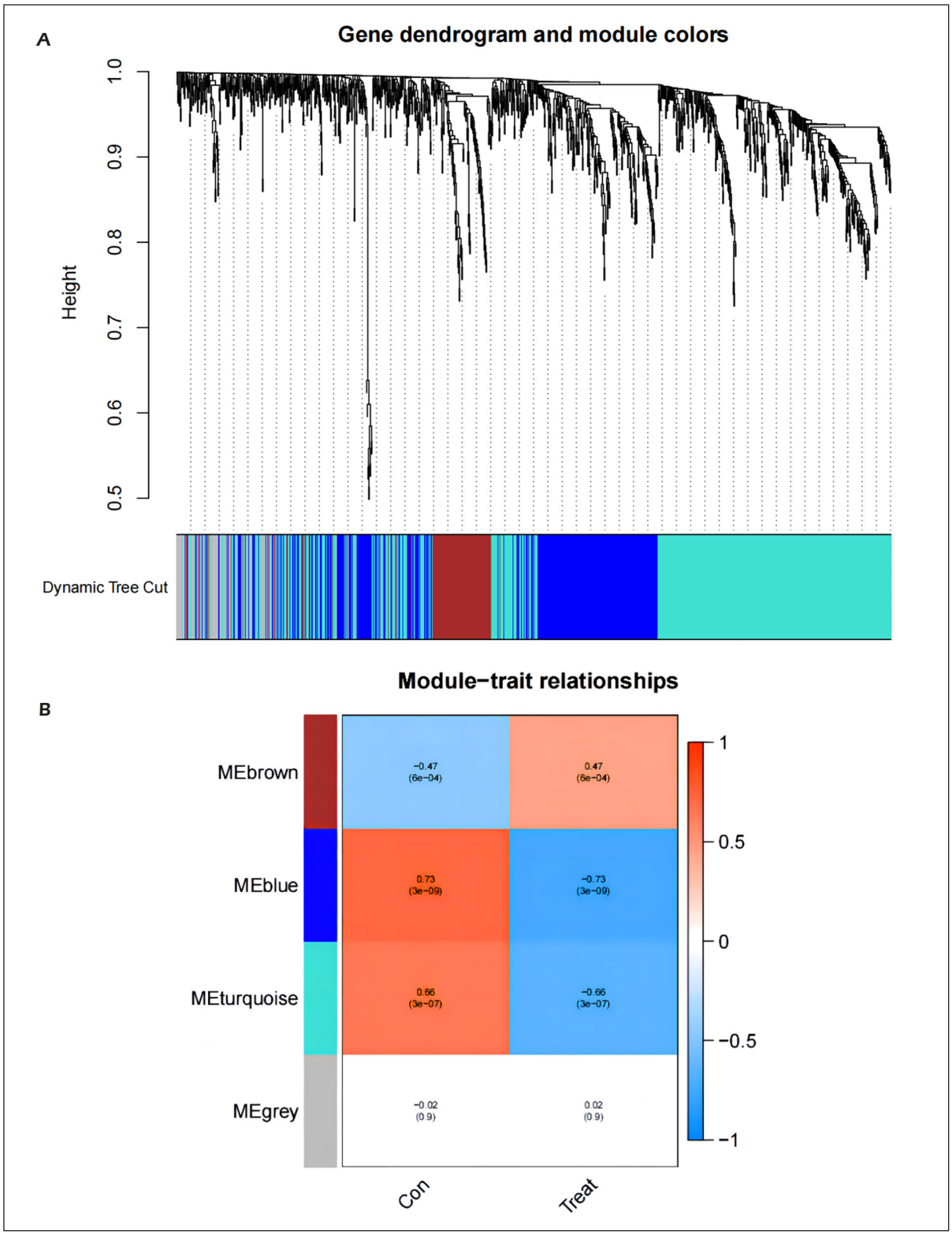

Figure 4. Dynamic identification clustering of modules and heat map of module-disease correlations: (**A**) gene dendrogram obtained by hierarchical clustering, where a row of colored bars below the tree diagram indicate the module assignment determined by dynamic tree cutting; (**B**) heat map of correlations between module feature genes and OA, in which the number above each cell indicates the corresponding correlation coefficient, the number in parentheses below is the test *p*-value, and the red and blue represent positive and negative correlations, respectively, while ME shows the module signature genes.

Table II. Core gene screening table.

Gene name	GS	MM
ATF3	0.79	0.83
COL14A1	0.63	0.83
COL3A1	0.53	0.84
FOSL2	0.61	0.83
GADD45B	0.55	0.87
KLF4	0.62	0.88
KLF9	0.66	0.84
LRRC17	0.55	0.83
MAFF	0.72	0.83
MXRA5	0.55	0.81
NFKBIA	0.64	0.88
NID2	0.60	0.84
PIGA	0.58	0.88
PPP1R15A	0.75	0.85
PTGDS	0.70	0.82
RHOB	0.65	0.91

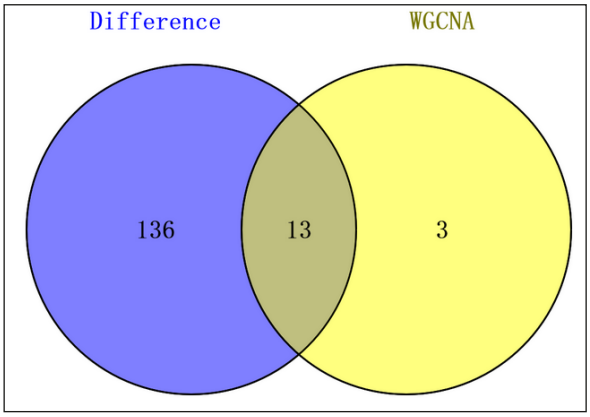

Figure 5. Venn diagram of differential genes *vs.* core genes: the blue part represents the number of differential genes, and the yellow part represents the number of core genes obtained by screening with the WGCNA algorithm.

of arthritis was often transient, instead of persistent, and it was significantly downregulated in the later stages of the disease. Their findings suggested the painful state of arthritis may have multiple neuropathic phenotypes, which indirectly suggests ATF3 is the main cause of pain in OA patients in the later stages. The results of this experiment were also validated by the low expression of ATF3 in the dataset obtained from this study, which was collected from patients with severe OA. Elsewhere, Chan et al[28] confirmed ATF3 plays an important role in influencing

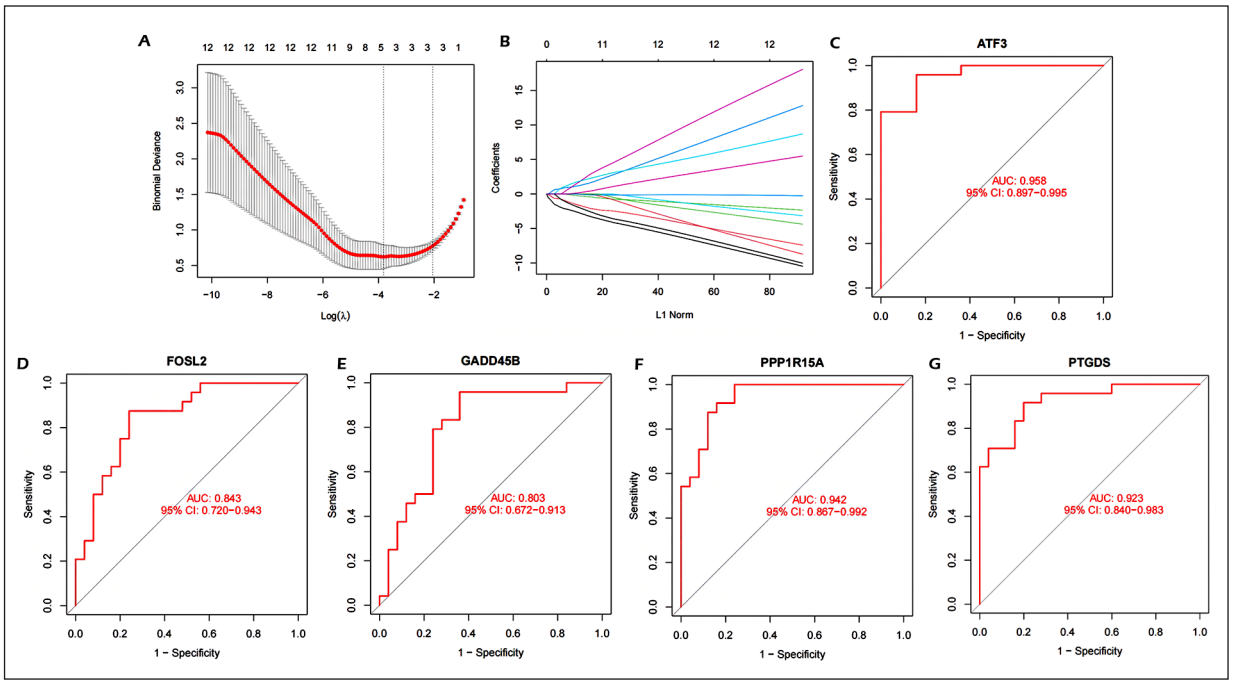

Figure 6. LASSO regression analysis method and ROC analysis results: (**A**) model cross-validation of the LASSO regression analysis method, in which two dashed lines correspond to two particular λ values: lambda.min; and lanbda.lse (left and right); (**B**) LASSO regression analysis method analysis for screening risk factors, where each curve in the graph represents the trajectory of 1 independent variable coefficient; (**C-G**) the results of ROC analysis for ATF, FOSL2, GADD45B, PPP1R15A, and PTGDS, respectively. The horizontal coordinate represents the false positive rate, while the vertical coordinate represents the sensitivity, i.e., the true positive rate. AUC is the area under the curve value.

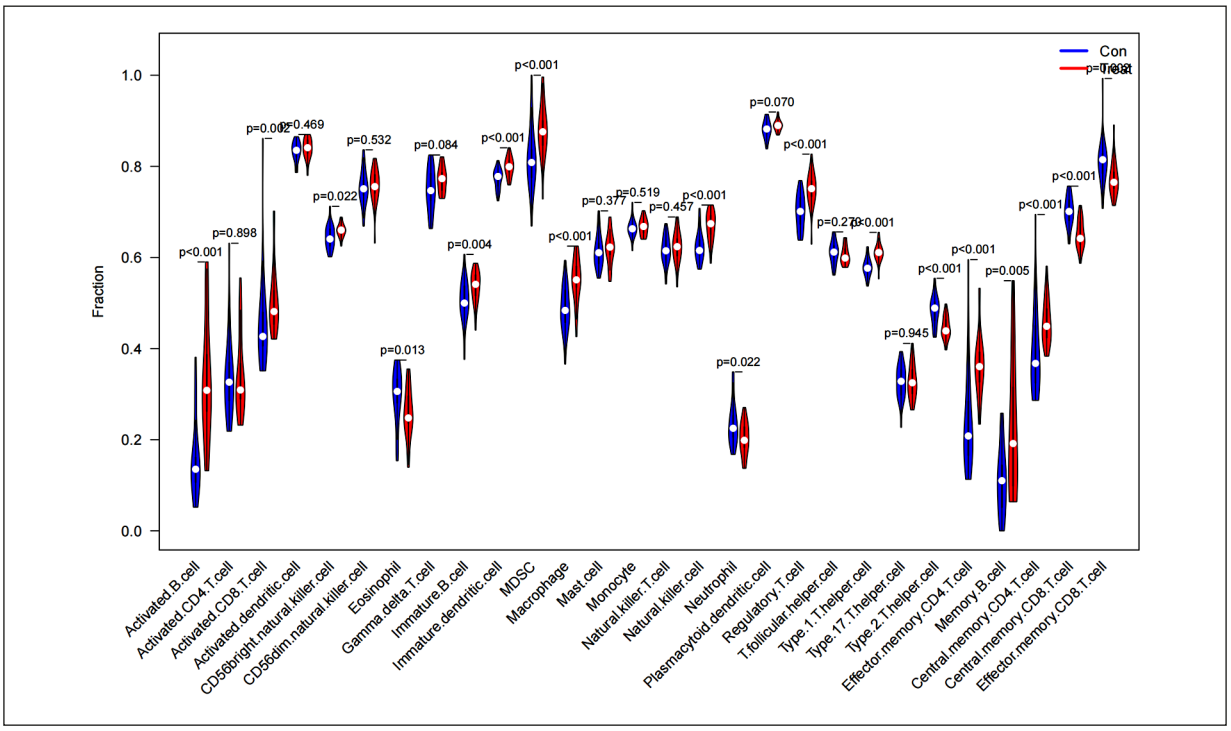

Figure 7. Graph of immune cell infiltration results: blue denotes the normal samples, while red denotes the OA samples, $p<0.05$ indicates significant difference, and the horizontal and vertical coordinates represent the 28 immune cells and their scores, respectively.

MMP13 expression after CFO transcription, and that it is transcriptionally dependent on the initial inflammation-induced expression of cFOS/cJUN. In experiments conducted on mice, ATF3 deficiency did not lead to skeletal abnormalities or affect cartilage formation but attenuated the progression of OA brought about by surgically induced knee instability[26]. This suggests ATF3 may play an important role in the treatment of early OA.

FOSL2 (also known as FRA2) is a FOS-associated protein of the AP-1 family, members of which can function by forming heterodimeric complexes with JUN proteins[29]. In this study, a

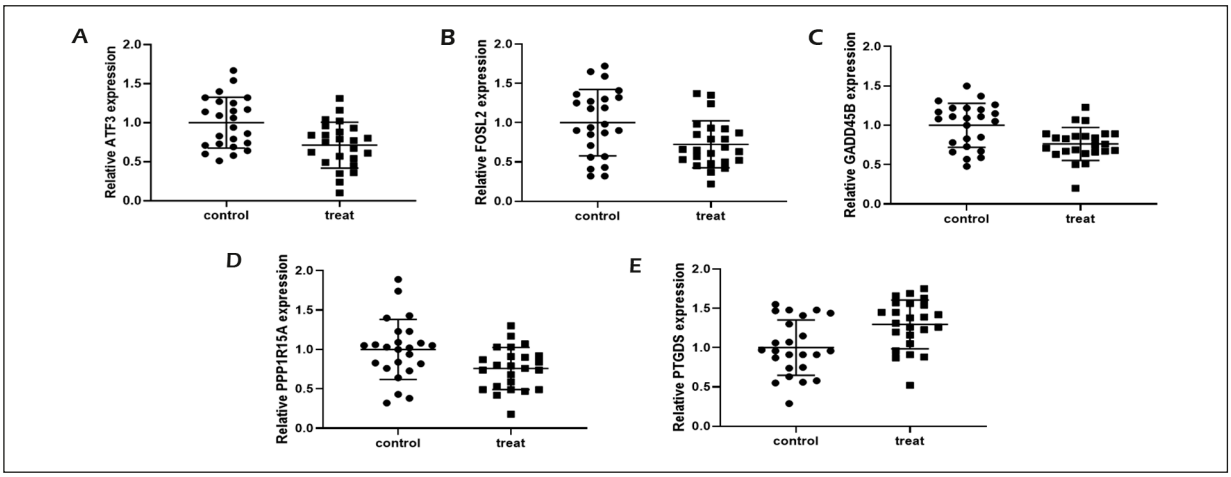

Figure 8. PCR graph results. **A-E,** They represent the expression of ATF3; FOSL2; GADD45B; PPP1R15A and PTGDS, respectively.

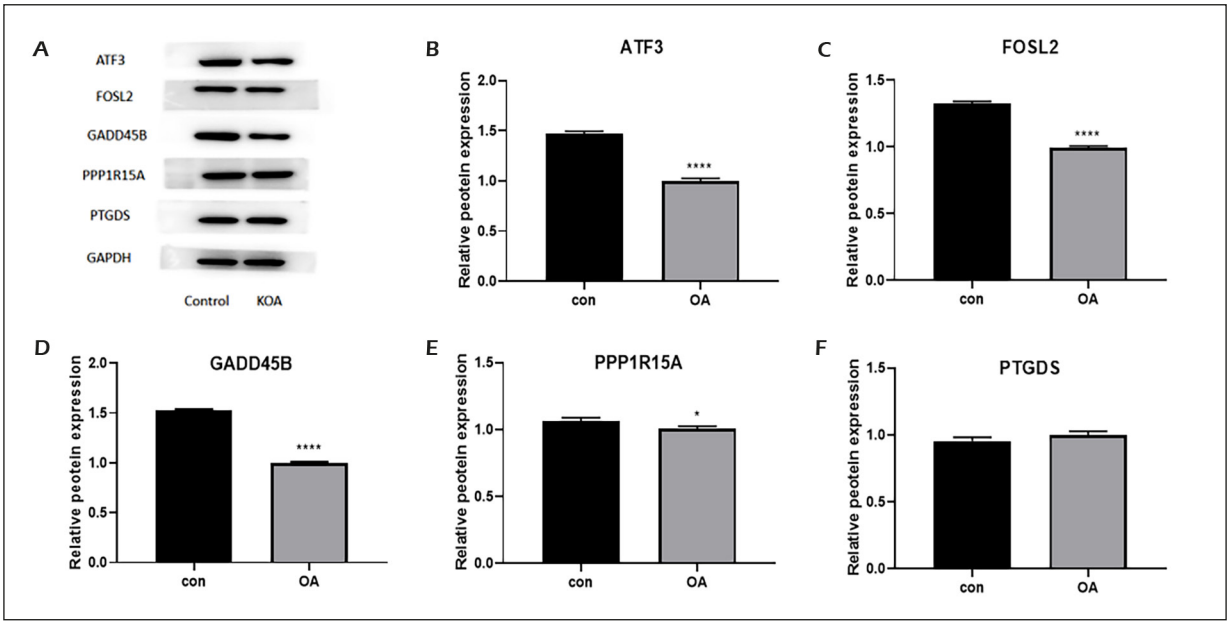

Figure 9. Protein expression maps. **A,** WB detection of relative expression of various proteins. **B-F,** They represent the protein expression of ATF3; FOSL2; GADD45B; PPP1R15A and PTGDS, respectively.

decrease of FOSL2 expression in chondrocytes of OA were observed. Previously, research concluded that FOSL2 plays a key role in inflammation-related diseases and activation of FOSL2/AP-1 induces a systemic inflammatory state. This increases both the infiltration of neutrophils and pro-inflammatory macrophages and the levels of pro-inflammatory cytokines such as TNF-α, IL-1β, and IL-6[30]. Fan et al[31] reported three subclasses of the mitogen-activated protein kinases (MAPKs): ERKs, JNKs, and p38 MAPK, play a key role in the induction of FOSL2/AP-1 activity, but the exact mechanism by which they regulate FOSL2 is not yet clear and requires further investigation. FOSL2 is also a key regulator of leptin expression in adipocytes[32], and its deficiency promotes obesity. In this study, FOSL2 was expressed at low levels in all cases of OA samples, which is also consistent with obesity being a major cause of OA. Previous studies have shown FOSL2 is repressed in the early hypertrophic state of chondrocytes, suggesting that this gene is closely associated with the early onset of OA[33], and that the regulation of FOSL2 is likely to have positive implications for the prevention of OA.

GADD45B is a member of a family of small molecule (18-kd) proteins which respond to genotoxic stress[34]. In recent research, GADD45B has been identified as an important mediator of BMP-2-induced early gene expression in chondrocytes and Col10α1 in late mouse embryonic mast chondrocytes[35]. It appears to have important effects on the progression of the early stages of OA. Relevantly, Tsuchimochi et al[36] reported that, early on, it activates the p38 MAPK pathway while other research has concluded GADD45B may activate C/EBPβ and thus form a positive feedback loop in chondrocytes, leading to cartilage degradation and bone redundancy[37]. In cell experiments, the use of GADD45B inhibitors can target the regulation of MAPK kinase 7 to inhibit endoplasmic reticulum stress and reduce chondrocyte apoptosis[38].Combined with the progress of current research, it may be stated GADD45B is closely related to early cartilage damage in OA.

However, the study presented here has some limitations. Firstly, because of the small sample size of the original dataset, even when data validation was performed, further suitable clinical samples are still needed for experimental validation. Secondly, this research was limited by certain conditions and further investigation could not be carried out on the role of core genes in the significant module. Furthermore, in the literature review, one of the findings was that the expression of ATF3 and GADD45B did not correlate linearly with disease progression. This suggests the two genes may play different roles

at different times in OA, but the lack of more direct and objective data did not allow arrival at any definitive conclusion. Therefore, more effort in refining the results of this study in the future is intended.

Conclusions

The results of this study suggest inflammation in cartilage tissue and the cellular stress response play crucial roles in how OA progresses. Bioinformatical analysis and validation suggest ATF3, FOSL2, and GADD45B may be genes of diagnostic and therapeutic value in osteochondropathy, but further molecular biology experiments are required for more rigorous verification of this.

Conflict of Interest

The author declare that the research was conducted in the absence of any commercial or financial relationships that could be construed as a potential conflict of interest.

Funding

This work was supported by the Youth Program of the National Natural Science Foundation of China (82104897); the Traditional Chinese Medicine Science and Technology Development Plan Project of Shandong (2019-0084); and the Natural Science Foundation of Shandong Province (ZR2020QH312, ZR2020MH099).

Authors' Contribution

Study design: WSQ, XWP; Statistical Analysis: WSQ, XWP, YL; Manuscript writing: WSQ; Manuscript modification: WSQ, YL. All authors read and approved the final manuscript.

Availability of Data and Materials

The datasets used and/or analyzed during the current study are available from the corresponding author on reasonable request.

Consent for Publication

All the authors approved the publication of this manuscript.

Ethics Approval

These experiments conformed to the Guide for the Care and Use of Laboratory Animals published by the National Institutes of Health. All animal experiments were approved by the Animal Ethics Committee of the Affiliated Hospital of Shandong University of Traditional Chinese Medicine (AWE-2021-04).

References

1) Pereira D, Ramos E, Branco J. Osteoarthritis. Acta Med Port 2015; 28: 99-106.
2) Hunter DJ, Bierma-Zeinstra S. Osteoarthritis. Lancet 2019; 393: 1745-1759.
3) Hunter DJ, March L, Chew M. Osteoarthritis in 2020 and beyond: a Lancet Commission. Lancet 2020; 396: 1711-1712.
4) Lin W, Wang Y, Chen Y, Wang Q, Gu Z, Zhu Y. Role of Calcium Signaling Pathway-Related Gene Regulatory Networks in Ischemic Stroke Based on Multiple WGCNA and Single-Cell Analysis. Oxid Med Cell Longev 2021; 2021: 8060477.
5) Langfelder P, Horvath S. WGCNA: an R package for weighted correlation network analysis. BMC Bioinformatics 2008; 9: 559.
6) Liu K, Chen S, Lu R. Identification of important genes related to ferroptosis and hypoxia in acute myocardial infarction based on WGCNA. Bioengineered 2021; 12: 7950-7963.
7) Lin W, Wang Y, Chen Y, Wang Q, Gu Z, Zhu Y. Role of Calcium Signaling Pathway-Related Gene Regulatory Networks in Ischemic Stroke Based on Multiple WGCNA and Single-Cell Analysis. Oxid Med Cell Longev 2021; 2021: 8060477.
8) Zhang X, Cui Y, Ding X, Liu S, Han B, Duan X, Zhang H, Sun T. Analysis of mRNA lncRNA and mRNA lncRNA-pathway co expression networks based on WGCNA in developing pediatric sepsis. Bioengineered 2021; 12: 1457-1470.
9) Tan R, Zhang G, Liu R, Hou J, Dong Z, Deng C, Wan S, Lai X, Cui H. Identification of Early Diagnostic and Prognostic Biomarkers via WGCNA in Stomach Adenocarcinoma. Front Oncol 2021; 11: 636461.
10) Hu RW, Liu C, Yan YY, Li D. Identification of hub genes and molecular subtypes in COVID-19 based on WGCNA. Eur Rev Med Pharmacol Sci 2021; 25: 6411-6424.
11) Haase F, Gloss BS, Tam PPL, Gold WA. WGCNA Identifies Translational and Proteasome-Ubiquitin Dysfunction in Rett Syndrome. Int J Mol Sci 2021; 22: 9954.
12) Voigt A, Almaas E. Assessment of weighted topological overlap (wTO) to improve fidelity of gene co-expression networks. BMC Bioinformatics 2019; 20: 58.
13) Xu M, Ouyang T, Lv K, Ma X. Integrated WGCNA and PPI Network to Screen Hub Genes Signatures for Infantile Hemangioma. Front Genet 2021; 11: 614195.
14) Wang Y, Chen L, Ju L, Qian K, Liu X, Wang X, Xiao Y. Novel Biomarkers Associated with Progression and Prognosis of Bladder Cancer Identified by Co-expression Analysis. Front Oncol 2019; 9: 1030.
15) Farhadian M, Rafat SA, Panahi B, Mayack C. Weighted gene co-expression network analysis identifies modules and functionally enriched pathways in the lactation process. Sci Rep 2021; 11: 2367.

16) Luo X, Feng L, Xu W, Bai X, Wu M. Weighted gene co-expression network analysis of hub genes in lung adenocarcinoma. Evol Bioinform Online 2021; 17: 11769343211009898.

17) McEligot AJ, Poynor V, Sharma R, Panangadan A. Logistic LASSO Regression for Dietary Intakes and Breast Cancer. Nutrients 2020; 12: 2652.

18) Jayadev C, Hulley P, Swales C, Snelling S, Collins G, Taylor P, Price A. Synovial fluid fingerprinting in end-stage knee osteoarthritis: a novel biomarker concept. Bone Joint Res 2020; 9: 623-632.

19) Kim Y, Kang JW, Kang J, Kwon EJ, Ha M, Kim YK, Lee H, Rhee JK, Kim YH. Novel deep learning-based survival prediction for oral cancer by analyzing tumor-infiltrating lymphocyte profiles through CIBERSORT. Oncoimmunology 2021; 10: 1904573.

20) Cao GM, Xuan XZ, Dong HL. Low expression of integrin signaling pathway genes is associated with abdominal aortic aneurysm: a bioinformatic analysis by WGCNA. Eur Rev Med Pharmacol Sci 2022; 6: 847-2860.

21) Hawker GA. Osteoarthritis is a serious disease. Clin Exp Rheumatol 2019; 37 Suppl 120: 3-6.

22) Bai KH, He SY, Shu LL, Wang WD, Lin SY, Zhang QY, Li L, Cheng L, Dai YJ. Identification of cancer stem cell characteristics in liver hepatocellular carcinoma by WGCNA analysis of transcriptome stemness index. Cancer Med 2020; 9: 4290-4298.

23) Conaghan PG, Cook AD, Hamilton JA, Tak PP. Therapeutic options for targeting inflammatory osteoarthritis pain. Nat Rev Rheumatol 2019; 15: 355-363.

24) Zhang H, Lin C, Zeng C, Wang Z, Wang H, Lu J, Liu X, Shao Y, Zhao C, Pan J, Xu S, Zhang Y, Xie D, Cai D, Bai X. Synovial macrophage M1 polarisation exacerbates experimental osteoarthritis partially through R-spondin-2. Ann Rheum Dis 2018; 77: 1524-1534.

25) Li X, Li Y, Yang X, Liao R, Chen L, Guo Q, Yang J. PR11-364P22.2/ATF3 protein interaction mediates IL-1β-induced catabolic effects in cartilage tissue and chondrocytes. J Cell Mol Med 2021; 25: 6188-6202.

26) Iezaki T, Ozaki K, Fukasawa K, Inoue M, Kitajima S, Muneta T, Takeda S, Fujita H, Onishi Y, Horie T, Yoneda Y, Takarada T, Hinoi E. ATF3 deficiency in chondrocytes alleviates osteoarthritis development. J Pathol 2016; 239: 426-437.

27) Blom AB, van den Bosch MH, Blaney Davidson EN, Roth J, Vogl T, van de Loo FA, Koenders M, van der Kraan PM, Geven EJ, van Lent PL. The alarmins S100A8 and S100A9 mediate acute pain in experimental synovitis. Arthritis Res Ther 2020; 22: 199.

28) Chan CM, Macdonald CD, Litherland GJ, Wilkinson DJ, Skelton A, Europe-Finner GN, Rowan AD. Cytokine-induced MMP13 Expression in Human Chondrocytes Is Dependent on Activating Transcription Factor 3 (ATF3) Regulation. J Biol Chem 2017; 292: 1625-1636.

29) Sarode P, Zheng X, Giotopoulou GA, Weigert A, Kuenne C, Günther S, Friedrich A, Gattenlöhner S, Stiewe T, Brüne B, Grimminger F, Stathopoulos GT, Pullamsetti SS, Seeger W, Savai R. Reprogramming of tumor-associated macrophages by targeting β-catenin/FOSL2/ARID5A signaling: A potential treatment of lung cancer. Sci Adv 2020; 6: eaaz6105.

30) Renoux F, Stellato M, Haftmann C, Vogetseder A, Huang R, Subramaniam A, Becker MO, Blyszczuk P, Becher B, Distler JHW, Kania G, Boyman O, Distler O. The AP1 Transcription Factor Fosl2 Promotes Systemic Autoimmunity and Inflammation by Repressing Treg Development. Cell Rep 2020; 31: 107826.

31) Fan S, Yin Q, Li D, Ma J, Li L, Chai S, Guo H, Yang Z. Anti-neuroinflammatory effects of Eucommia ulmoides Oliv. In a Parkinson's mouse model through the regulation of p38/JNK-Fosl2 gene expression. J Ethnopharmacol 2020; 260: 113016.

32) Wrann CD, Eguchi J, Bozec A, Xu Z, Mikkelsen T, Gimble J, Nave H, Wagner EF, Ong SE, Rosen ED. FOSL2 promotes leptin gene expression in human and mouse adipocytes. J Clin Invest. 2012; 122: 1010-21.

33) He X, Ohba S, Hojo H, McMahon AP. AP-1 family members act with Sox9 to promote chondrocyte hypertrophy. Development 2016; 143: 3012-3023.

34) Svensson CI, Inoue T, Hammaker D, Fukushima A, Papa S, Franzoso G, Schett G, Corr M, Boyle DL, Firestein GS. Gadd45beta deficiency in rheumatoid arthritis: enhanced synovitis through JNK signaling. Arthritis Rheum 2009; 60: 3229-3240.

35) Ijiri K, Zerbini LF, Peng H, Otu HH, Tsuchimochi K, Otero M, Dragomir C, Walsh N, Bierbaum BE, Mattingly D, van Flandern G, Komiya S, Aigner T, Libermann TA, Goldring MB. Differential expression of GADD45beta in normal and osteoarthritic cartilage: potential role in homeostasis of articular chondrocytes. Arthritis Rheum 2008; 58: 2075-2087.

36) Tsuchimochi K, Otero M, Dragomir CL, Plumb DA, Zerbini LF, Libermann TA, Marcu KB, Komiya S, Ijiri K, Goldring MB. GADD45beta enhances Col10a1 transcription via the MTK1/MKK3/6/p38 axis and activation of C/EBPbeta-TAD4 in terminally differentiating chondrocytes. J Biol Chem 2010; 285: 8395-8407.

37) Shimada H, Otero M, Tsuchimochi K, Yamasaki S, Sakakima H, Matsuda F, Sakasegawa M, Setoguchi T, Xu L, Goldring MB, Tanimoto A, Komiya S, Ijiri K. CCAAT/enhancer binding protein β (C/EBPβ) regulates the transcription of growth arrest and DNA damage-inducible protein 45 β (GADD45β) in articular chondrocytes. Pathol Res Pract 2016; 212: 302-309.

38) Zhang Z, Li M, Ma X, Zhou SL, Ren ZW, Qiu YS. GADD45β-I attenuates oxidative stress and apoptosis via Sirt3-mediated inhibition of ER stress in osteoarthritis chondrocytes. Chem Biol Interact 2018; 296: 76-82.